Electronic Supplementary Material (ESI) for New Journal of Chemistry.

New Journal of Chemistry - Electronic Supplementary Information

Metal complexes with bis(2-pyridyl)diselenoethers: Structural chemistry and catalysis

Roberta Cargnelutti,[a] Felipe Dornelles da Silva,[a] Ulrich Abram[*b] and Ernesto Schulz Lang,[*a]

Table S1. Crystallographic data and refinement parameters for **1-6**.

Crystal Data	**1**	**2**	**3**	**4**	**5**	**6**
Formula	$C_{11}H_{10}Cl_2CuN_2Se_2$	$C_{22}H_{20}Cu_4I_4N_4Se_4$	$C_{26}H_{28}Cl_2CuN_4Se_4$	$C_{13}H_{14}Cl_2CoN_2Se_2$	$C_{13}H_{14}Ag\ N_3O_3Se_2$	$C_{14}H_{16}Cl_2CuN_2Se_2$
Fw (g mol^{-1})	462.57	1418.02	846.83	846.83	526.06	504.65
T (K)	173(2)	173(2)	200(2)	200(2)	200(2)	173(2)
Crystal system	Orthorhombic	Triclinic	Triclinic	Monoclinic	Monoclinic	Orthorhombic
Space group	$Pbca$	$P\bar{1}$	$P\bar{1}$	$P2_1/n$	$P2/c$	Pbca
a/Å	11.9328(10)	9.0860(2)	8.2538(10)	20.476(2)	9.7910(10)	10.2403(3)
b/Å	12.2111(10)	9.1684(2)	8.7192(10)	8.5749(6)	4.4420(10)	11.4552(3)
c/Å	18.6534(16)	10.5159(3)	11.6817(12)	21.202(2)	20.883(3)	14.8043(4)
α/°	90	70.960(10)	87.058(9)	90	90	90
β/°	90	88.276(10)	81.017(9)	115.735(8)	90.960	90
γ/°	90	77.370(10)	62.798(8)	90	90	90
V/Å^3	2718.0(4)	807.25(3)	738.35(14)	3353.4(6)	908.1(3)	1736.61(8)
Z	8	1	1	8	2	4
D_{calc} (g cm^{-3})	2.261	2.917	1.905	1.925	1.924	1.930
μ (Mo Kα) (mm^{-1})	7.337	10.954	5.874	5.674	5.130	5.751
λ/Å	0.71073	0.71073	0.71073	0.71073	0.71073	0.71073
F (000)	1768	644	411	1880	504	980
Collected reflns.	56282	11123	8469	18299	6289	27397
Unique reflns.	6021	7012	3933	6569	2433	3280
GOF (F^2)	0.852	1.053	0.781	0.717	0.947	1.014
$R_1{}^a$	0.0203	0.0193	0.0357	0.0479	0.0572	0.0217
$wR_2{}^b$	0.0924	0.0475	0.1060	0.0512	0.1522	0.0515

$^a R_1 = \sum \|F_o\| - \|F_c\| / \sum \|F_o\|$.

$^b wR_2 = \{\sum w(F_o{}^2 - F_c{}^2)^2/\sum w(F_o{}^2)^2\}^{1/2}$.

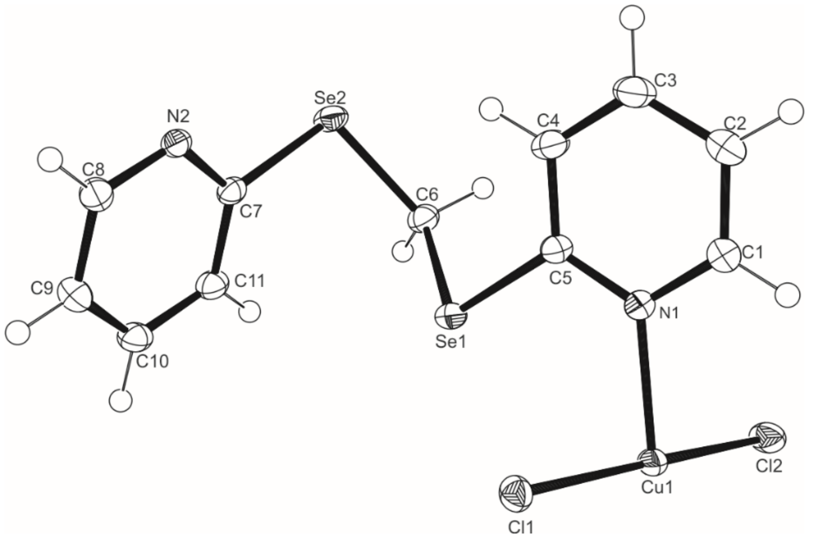

Figure S1. ORTEP[1] view of the asymmetric unit of the compound $[CuCl_2(L1)]_n$ (**1**) with the thermal ellipsoids at 50% probability. Selected bond lengths [Å] and angles [°]: Cu(1)−N(1) = 2.0644(15), Cu(1)−Cl(2) = 2.2493(5), Cu(1)-Cl(1) = 2.2757(5), Se(1)−C(5) = 1.9080(17), Se(1)−C(6) = 1.9513(18), Se(2)−C(7) = 1.8997(17), Se(2) −C(6) = 1.9567(17), N(1)−Cu(1)−Cl(1) = 90.67(4), Cl(1)−Cu(1)−Cl(2) = 175.91 (2).

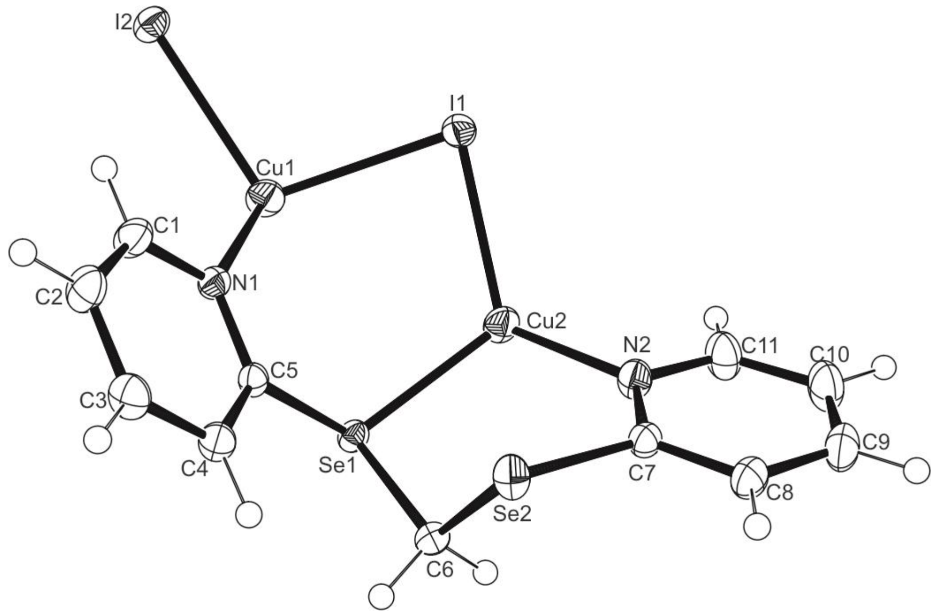

Figure S2. ORTEP[1] view of the asymmetric unit of the compound $[Cu_4I_4(L1)_2]$ (**2**) with the thermal ellipsoids at 50% probability. Selected bond distances [Å] and angles [º]: I(1)−Cu(2) = 2.5703(3), I(1)−Cu(1) = 2.6897(3), Cu(2)−N(2) = 2.0570(16), Cu(2)−Se(1) = 2.4240(3), I(2)−Cu(1) = 2.6890(3), Se(1)−C(5) = 1.9197(15), Cu(1)−N(1) = 2.0661(14), Cu(2)−I(1)−Cu(1) = 83.536(8), N(2)−Cu(2)−Se(1) = 110.29(4), N(2)−Cu(2)−I(1) = 118.35(5), Se(1)−Cu(2)−I(1) = 113.437(10), I(2)−Cu(1)−I(1) = 103.863(9).

[1] Farrujia, L.J. *"ORTEP 3 Program for Ellipsoid of Crystal Structures" J. Appl. Cryst*. **1997**, *30*.

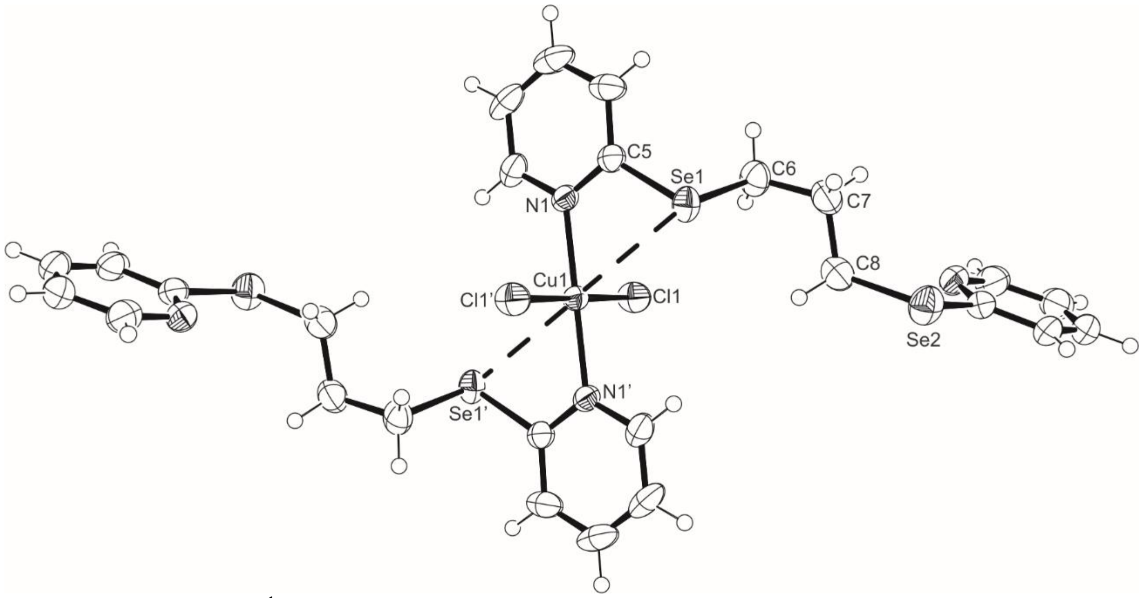

Figure S3. ORTEP[1] view of the asymmetric unit of the compound [$CuCl_2(L2)_2$] (**3**) with the thermal ellipsoids at 50% probability. Selected bond distances [Å] and angles [°]: Cu(1)−N(1) = 1.993(3), Cu(1)−Cl(1) = 2.2794(8), Cu(1)−Se(1) = 3.1289(3), N(1)−Cu(1)−Se(1) = 60.616(5), Cl(1)−Cu(1)−Se(1) = 91.491(6), N(1)−Cu(1)−Cl(1) = 91.18(8). Symmetry transformations used to generate equivalent atoms: (') 1−x, 1−y, 1−z.

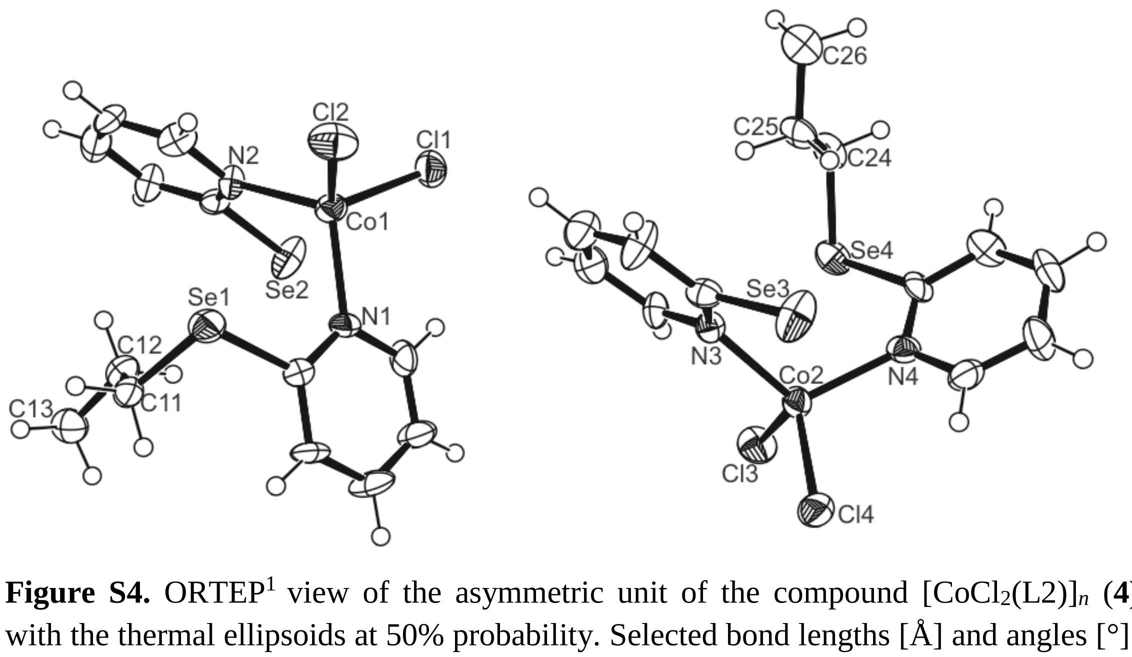

Figure S4. ORTEP[1] view of the asymmetric unit of the compound [$CoCl_2(L2)]_n$ (**4**) with the thermal ellipsoids at 50% probability. Selected bond lengths [Å] and angles [°]: Co(1)−N(1) = 2.052(6), Co(1)−N(2) = 2.053(6), Co(1)−Cl(1) = 2.247(2), Co(1)−Cl(2) = 2.252(2), N(1)−Co(1)−N(2) = 111.3(3), N(1)−Co(1)−Cl(1) = 105.44(18), N(2)−Co(1)−Cl(1) = 110.99(18), N(1)−Co(1)−Cl(2) = 113.78(18), N(2)−Co(1)−Cl(2) = 108.39(17), Cl(1)−Co(1)−Cl(2) = 106.87(10).

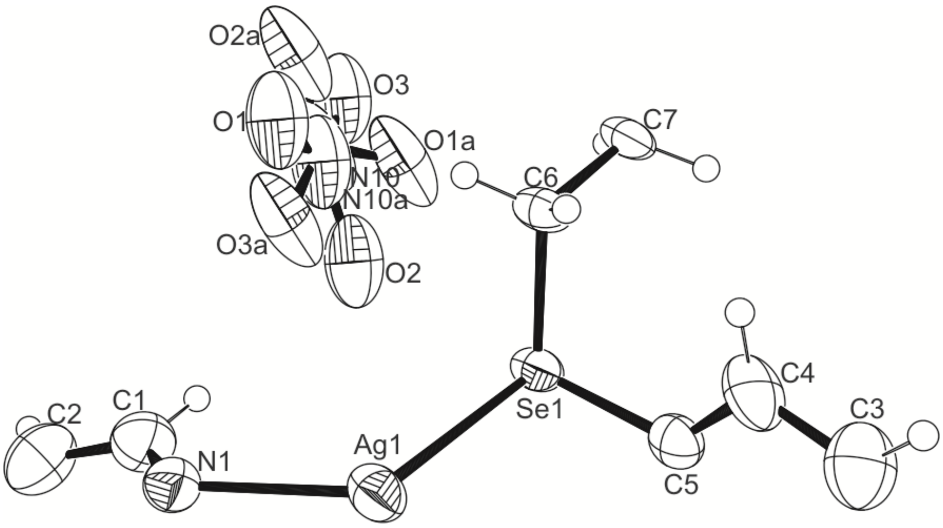

Figure S5. ORTEP[1] view of the asymmetric unit of the compound $[Ag(L2)(NO_3)]_n$ (**5**) with the thermal ellipsoids at 50% probability. The NO_3^- ion exhibit positional disorder. Selected bond distances [Å] and angles [º]: Se(1)−Ag(1) = 2.7310(6), Ag(1)−N(1) = 2.321(4), Se(1)–C(5) = 1.921(4), Se(1)–C(6) = 1.973(4), N(1)−Ag(1)−Se(1) = 123.37(9), C(6)–Se(1)–Ag(1) = 104.02(11), C(5)–Se(1)–Ag(1) = 93.98(12).

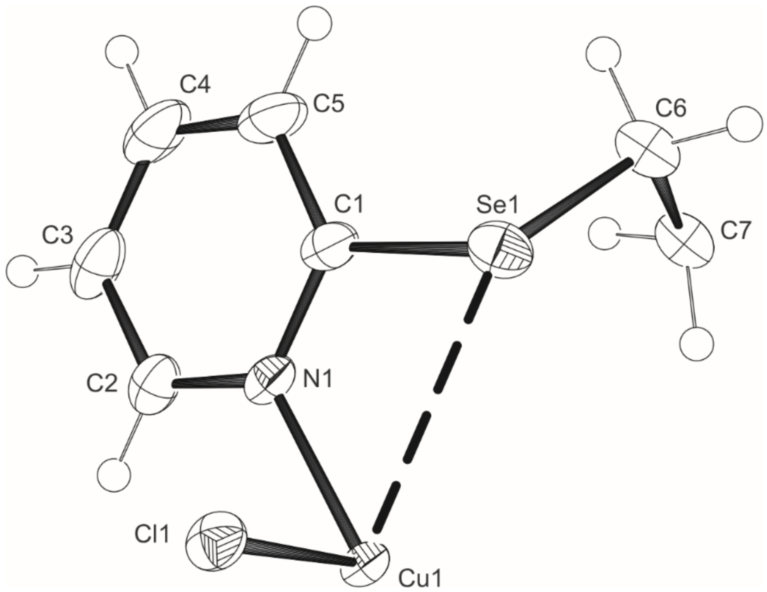

Figure S6. ORTEP[1] view of the asymmetric unit of the compound $[CuCl_2(L3)]_n$ (**6**) with the thermal ellipsoids at 50% probability. Selected bond lengths [Å] and angles [°]: Cu(1)−N(1) = 1.9762(11), Cu(1)−Cl(1) = 2.2861(3), Cu(1)−Se(1) = 3.0628(1); N(1)−Cu(1)−Se(1) = 82.118(1), Cl(1)−Cu(1)−Se(1) = 117.576(1), N(1)−Cu(1)−Cl(1) = 88.94(3).

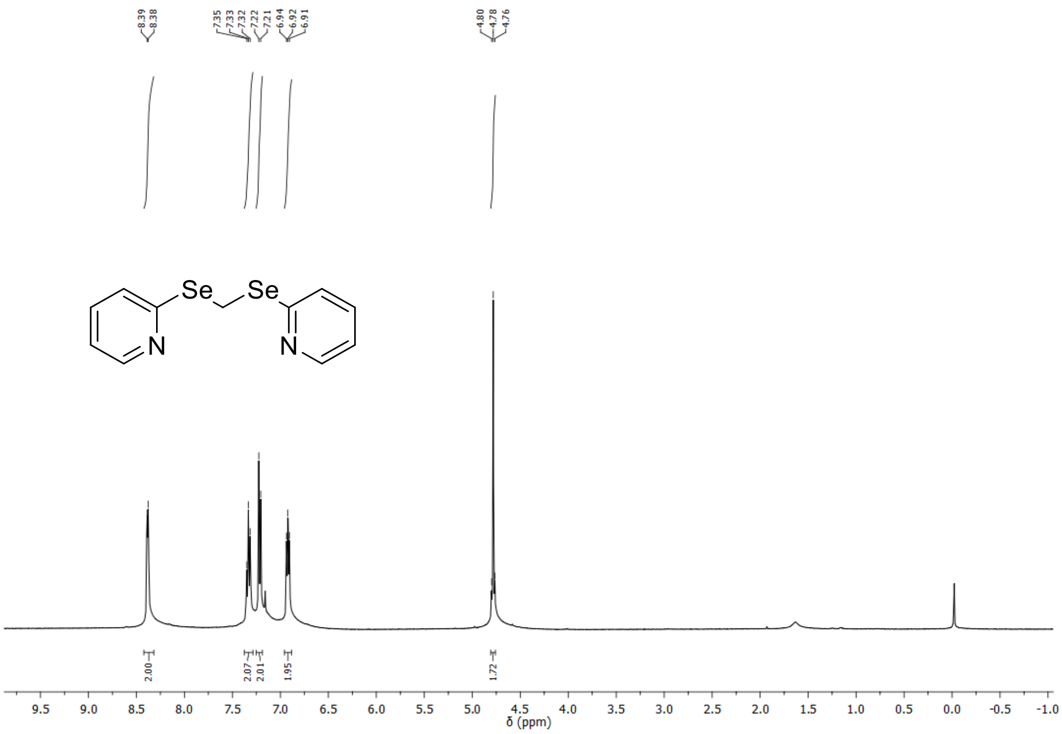

Figure S7. ^{1}H-NMR spectrum of Ligand (**L1**) in $CDCl_3$.

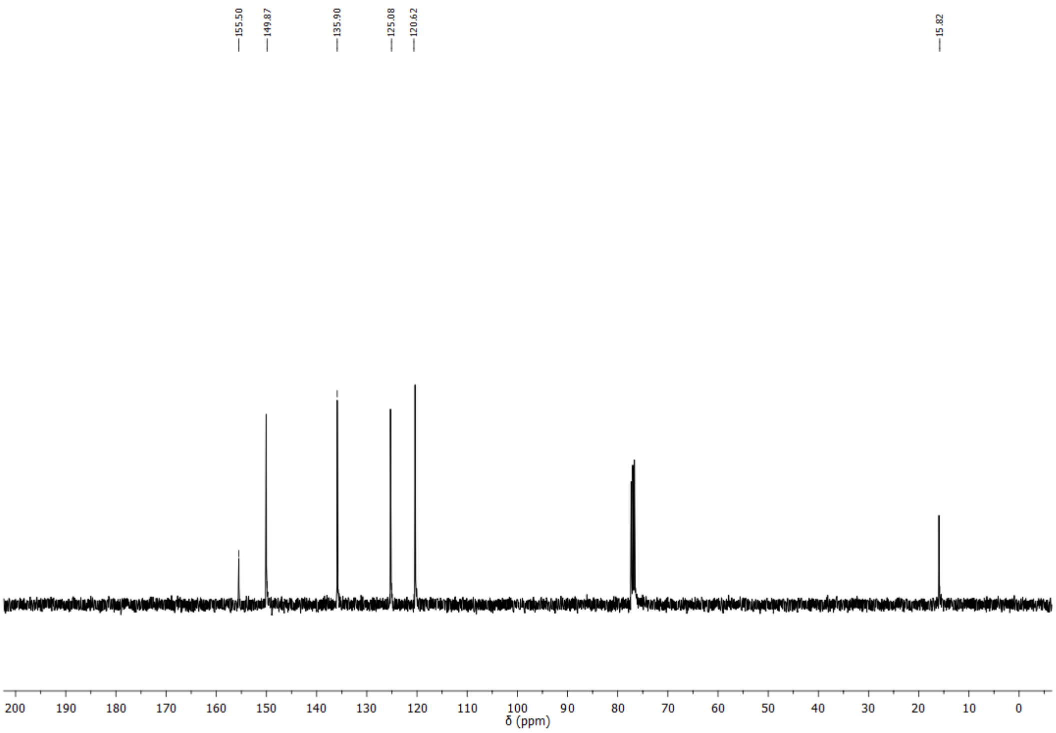

Figure S8. ^{13}C-NMR spectrum of Ligand (**L1**) in $CDCl_3$.

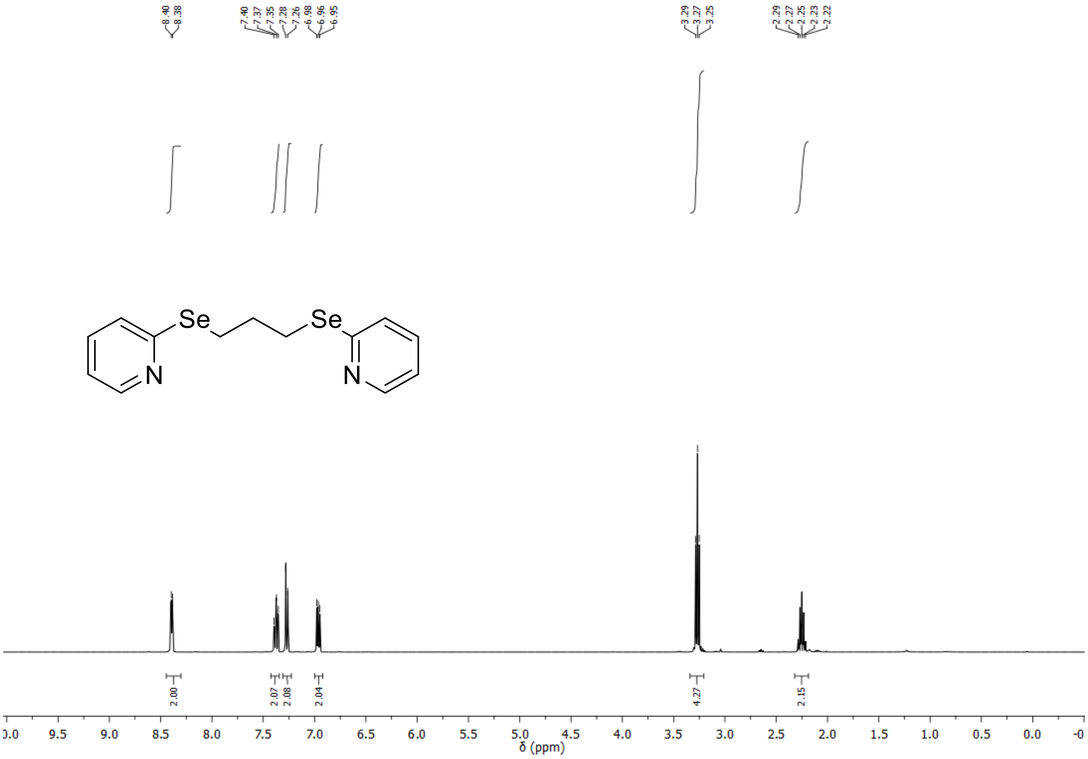

Figure S9. ^{1}H-NMR spectrum of Ligand (**L2**) in $CDCl_3$.

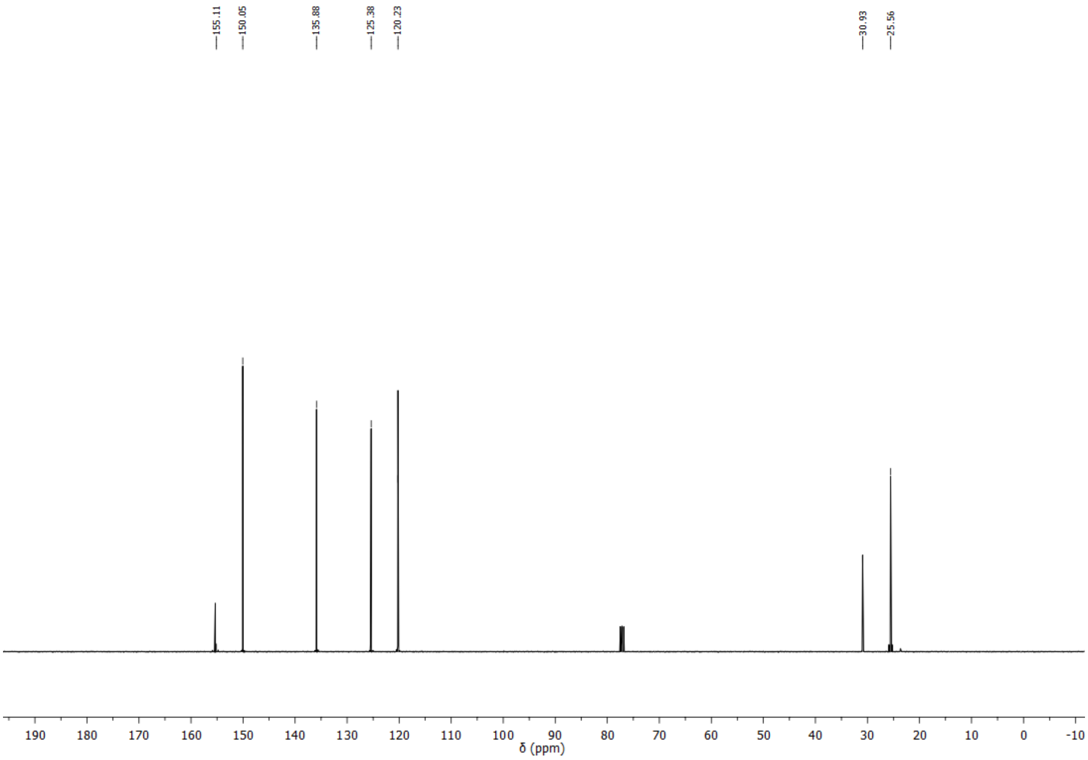

Figure S10. ^{13}C-NMR spectrum of Ligand (**L2**) in $CDCl_3$.

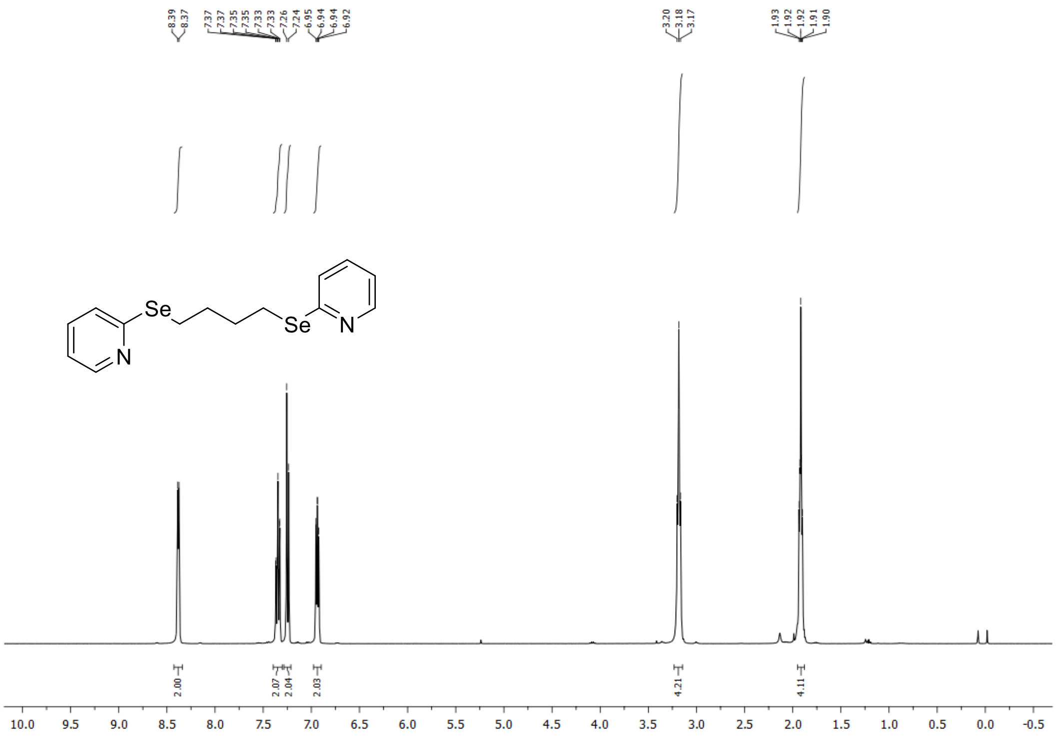

Figure S11. ^{1}H-NMR spectrum of Ligand (**L3**) in $CDCl_3$.

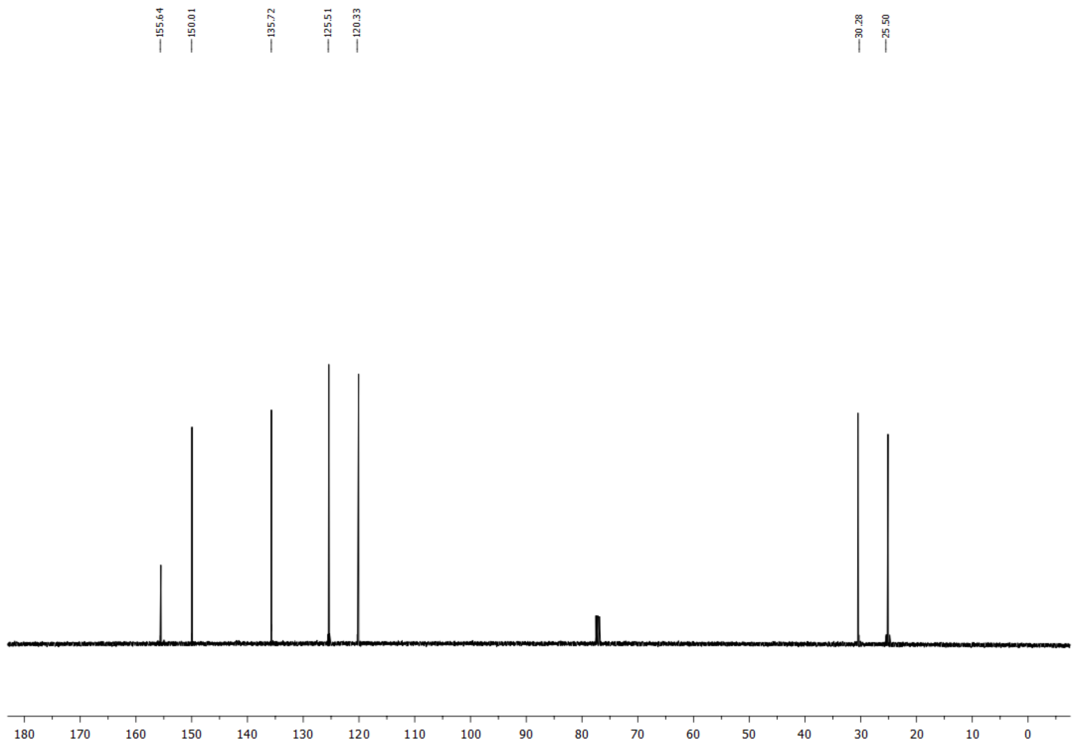

Figure S12. ^{13}C-NMR spectrum of Ligand (**L3**) in $CDCl_3$.

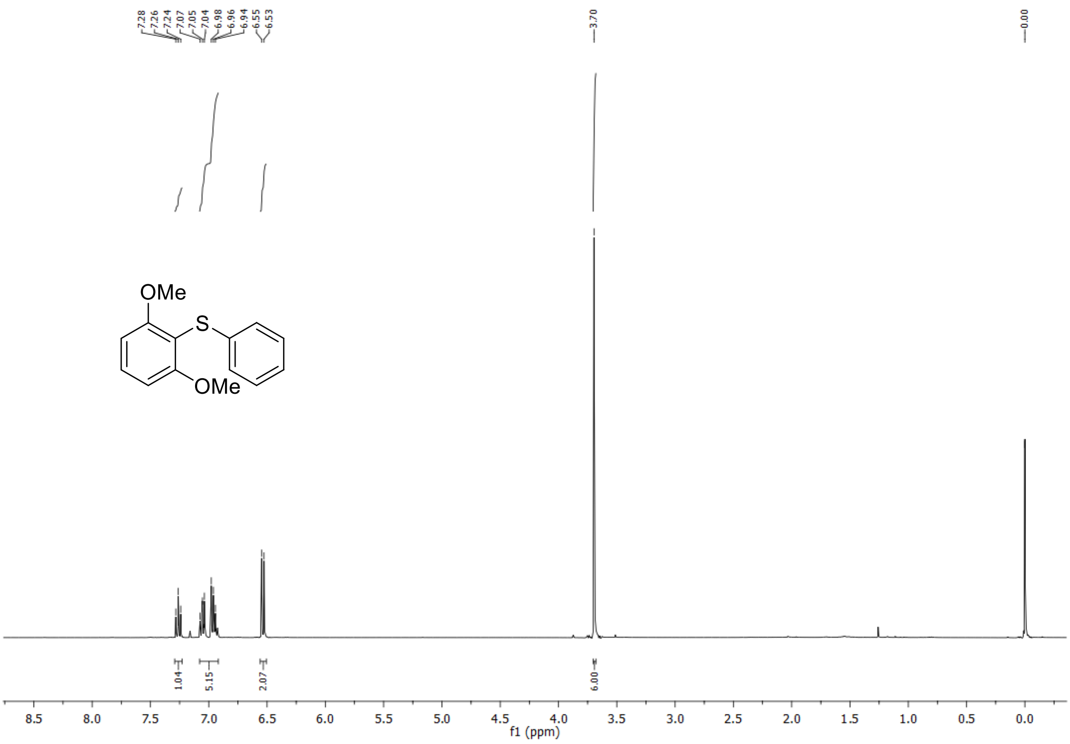

Figure S13. ^{1}H-NMR spectrum of **9a** in $CDCl_3$.

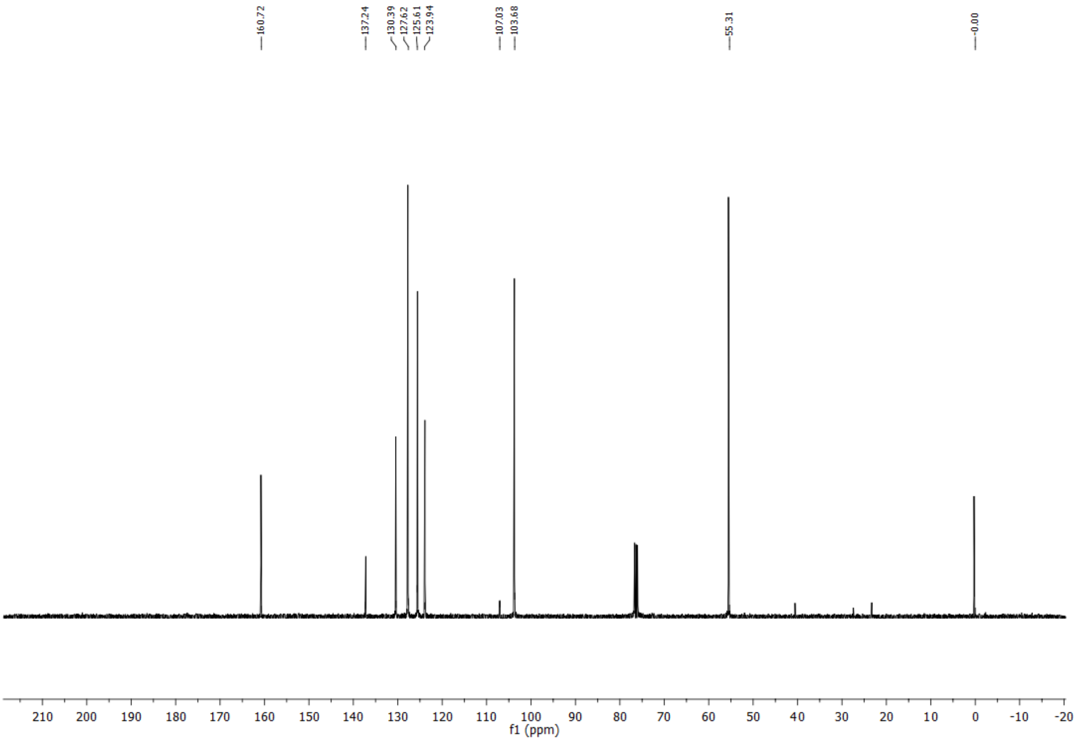

Figure S14. ^{13}C-NMR spectrum of **9a** in $CDCl_3$.

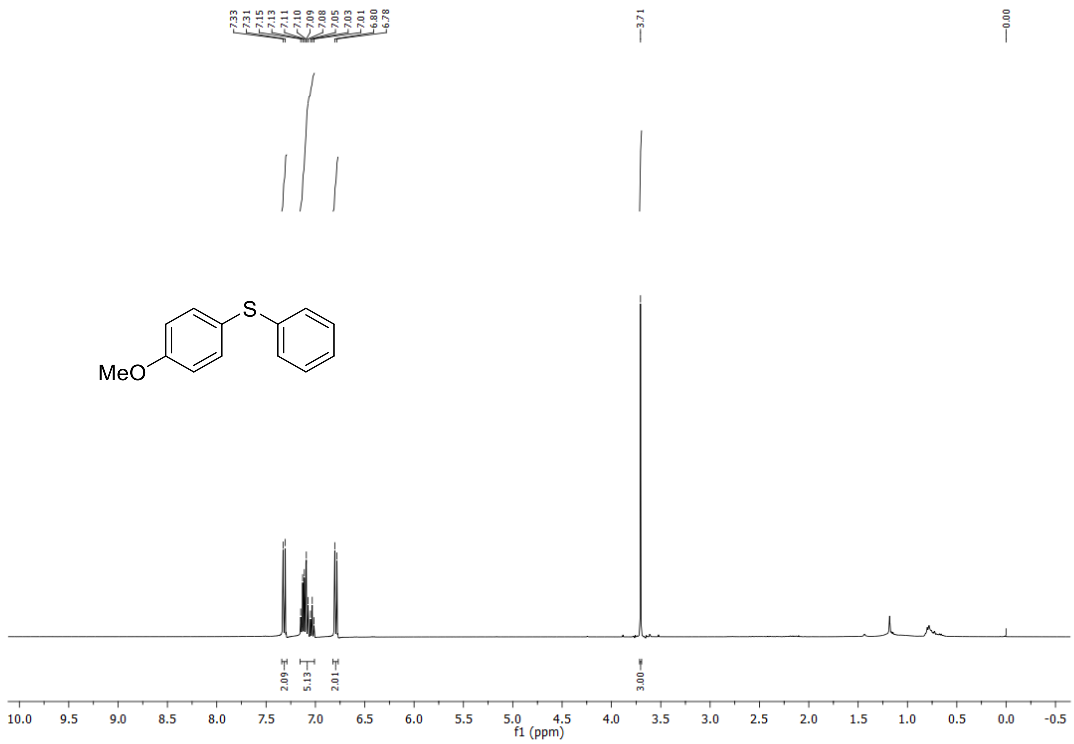

Figure S15. ^{1}H-NMR spectrum of **9b** in $CDCl_3$.

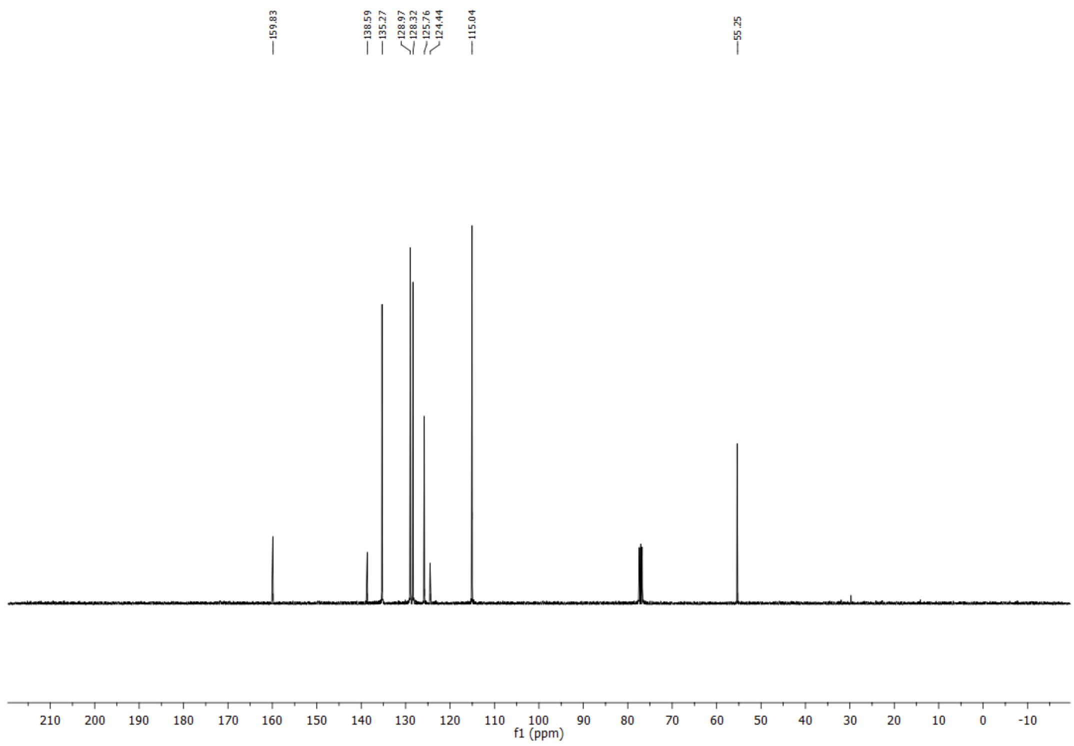

Figure S16. ^{13}C-NMR spectrum of **9b** in $CDCl_3$.

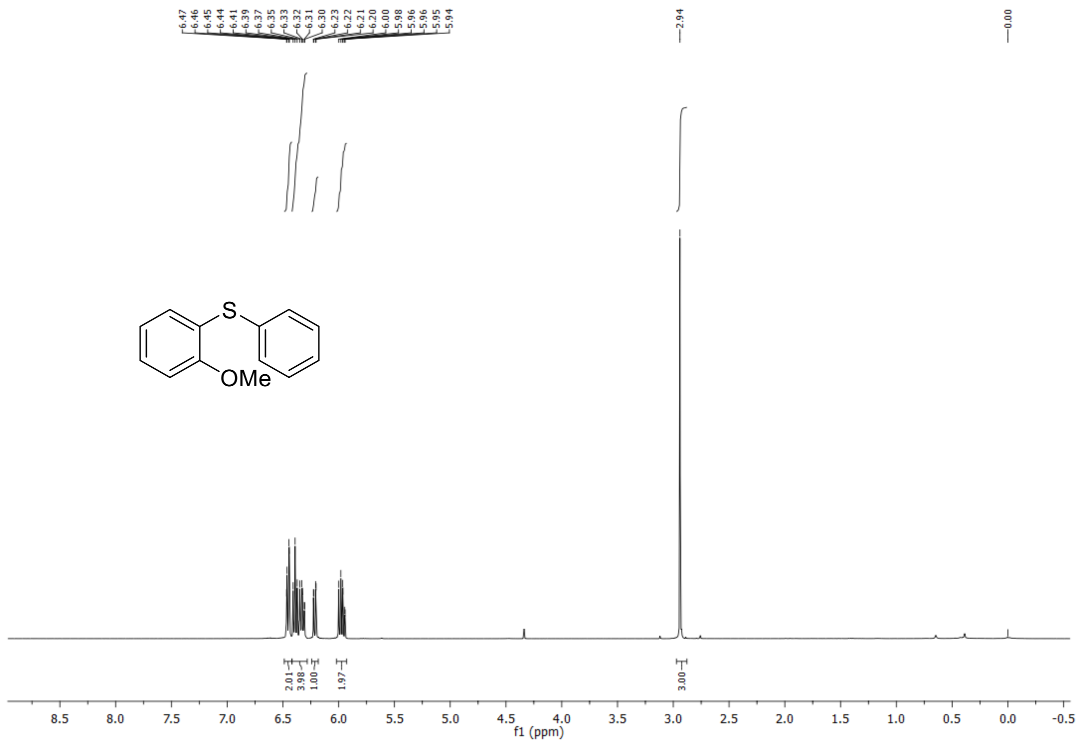

Figure S17. ^{1}H-NMR spectrum of **9c** in $CDCl_3$.

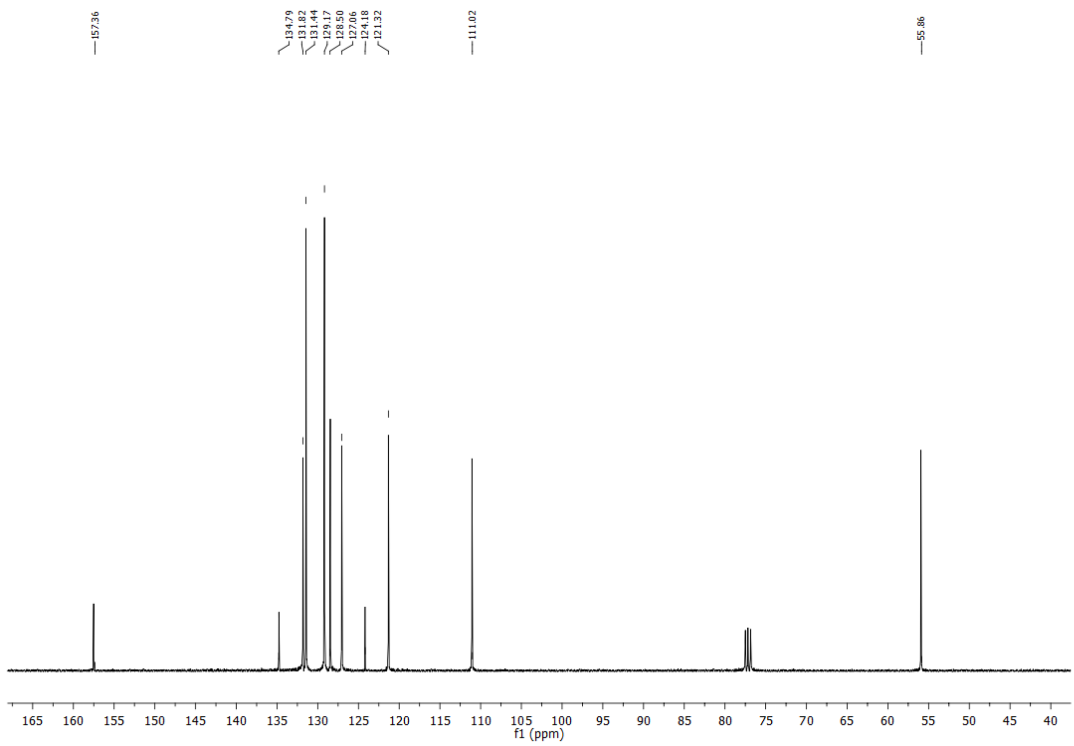

Figure S18. ^{13}C-NMR spectrum of **9c** in $CDCl_3$.

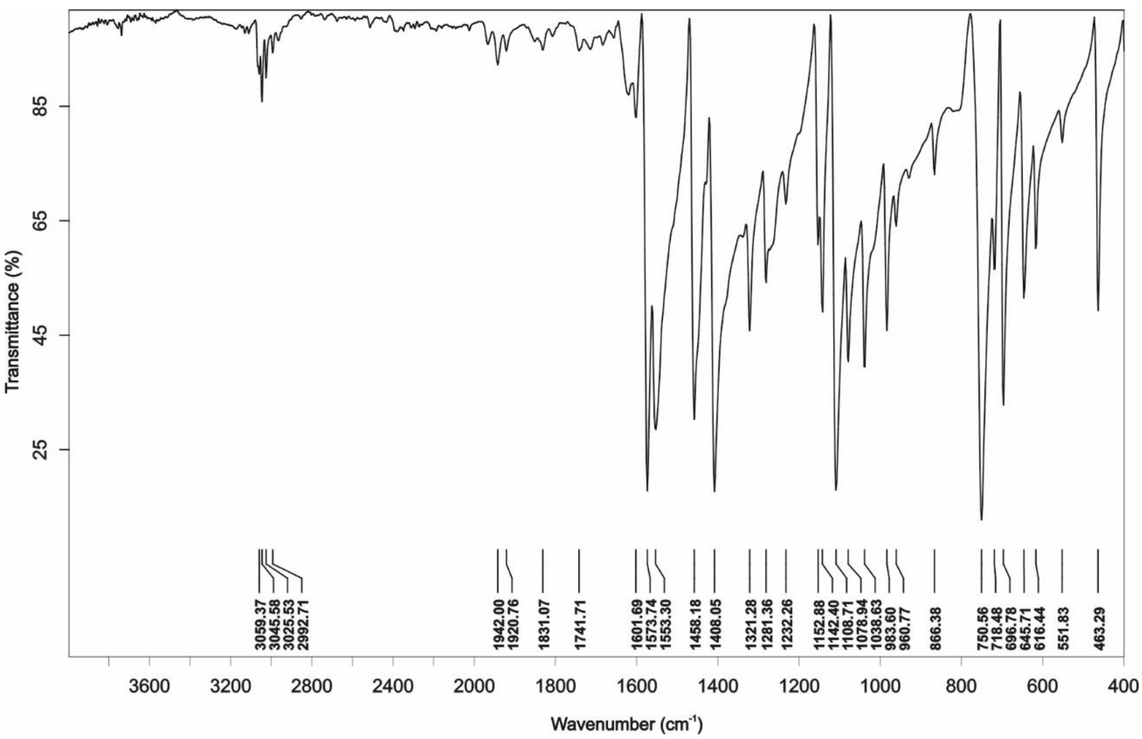

Figure S19. FT-IR spectrum of [(Py'Se)$_2$(CH$_2$)] (**L1**).

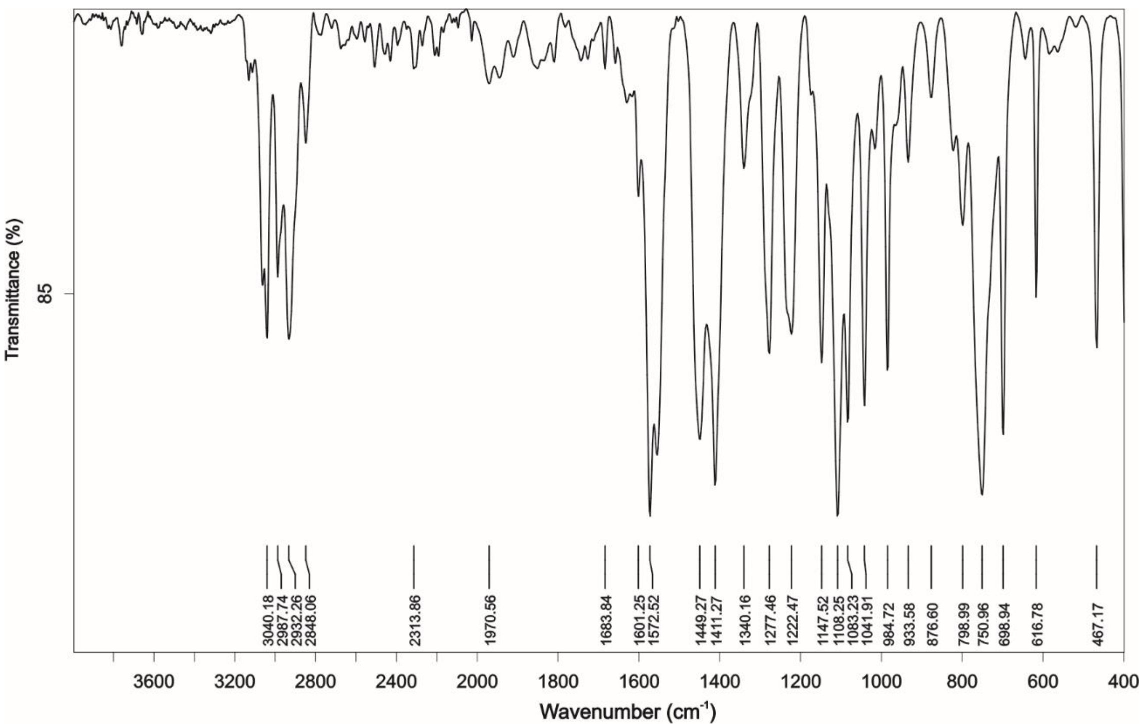

Figure S20. FT-IR spectrum of [(Py'Se)$_2$(C$_3$H$_6$)] (**L2**).

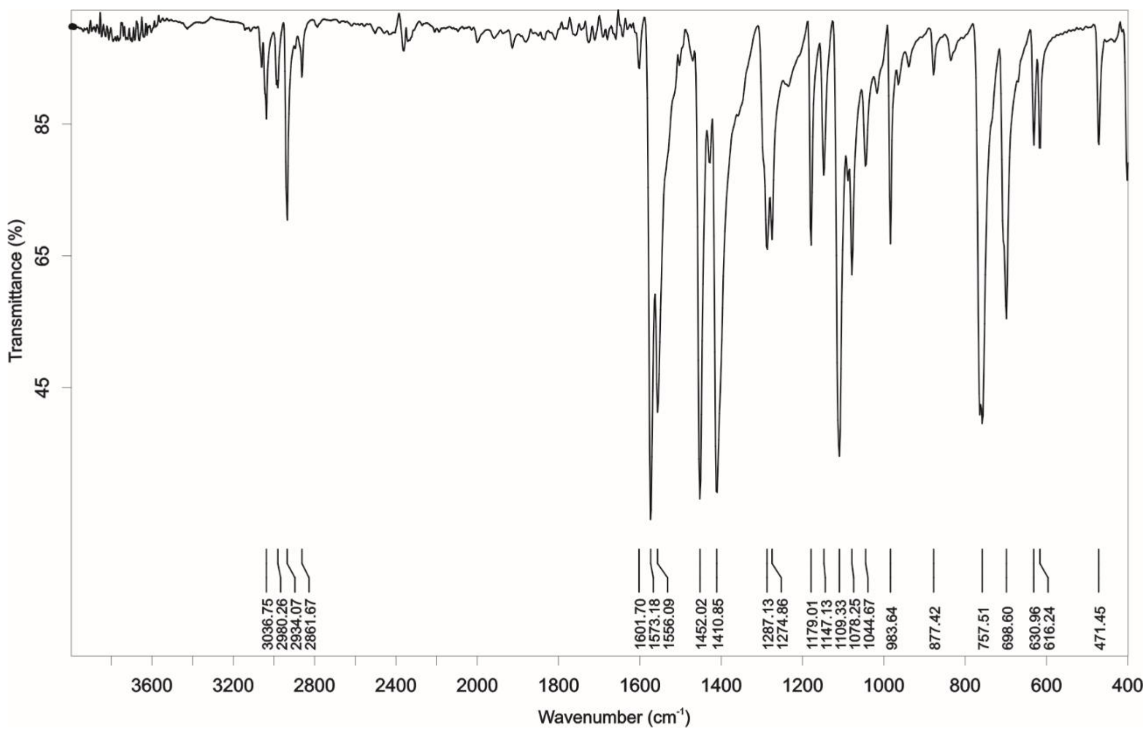

Figure S21. FT-IR spectrum of [(Py'Se)$_2$(C$_4$H$_8$)] (**L3**).

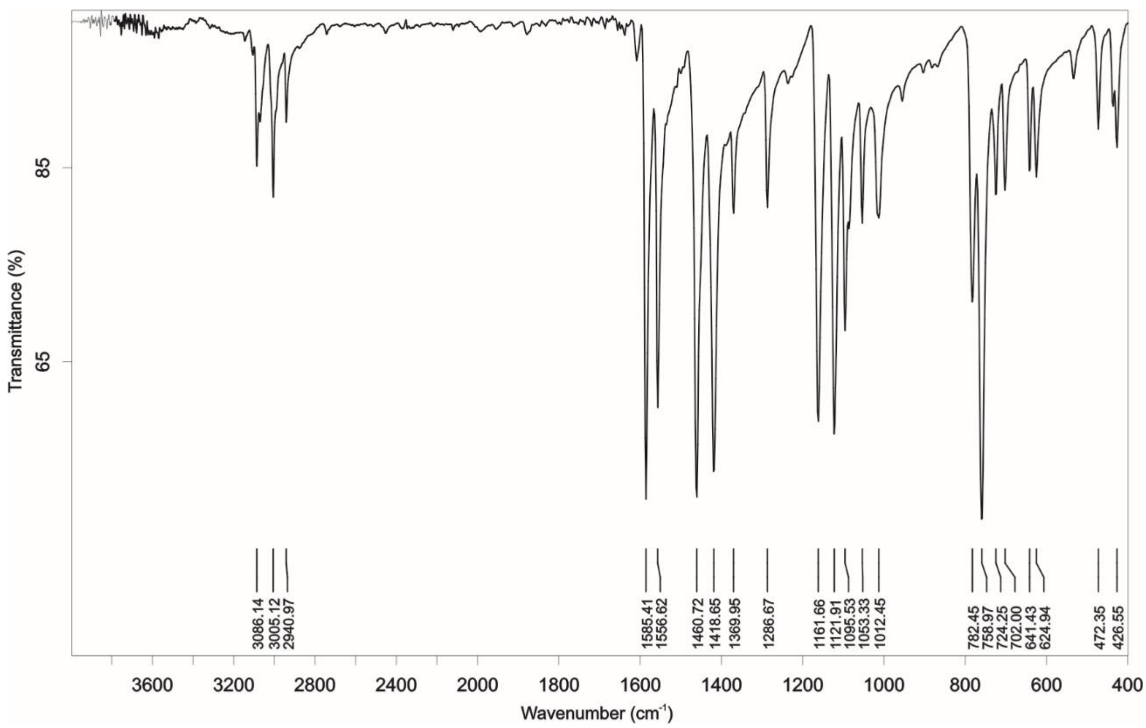

Figure S22. FT-IR spectrum of [CuCl$_2$(L1)]$_n$ (**1**).

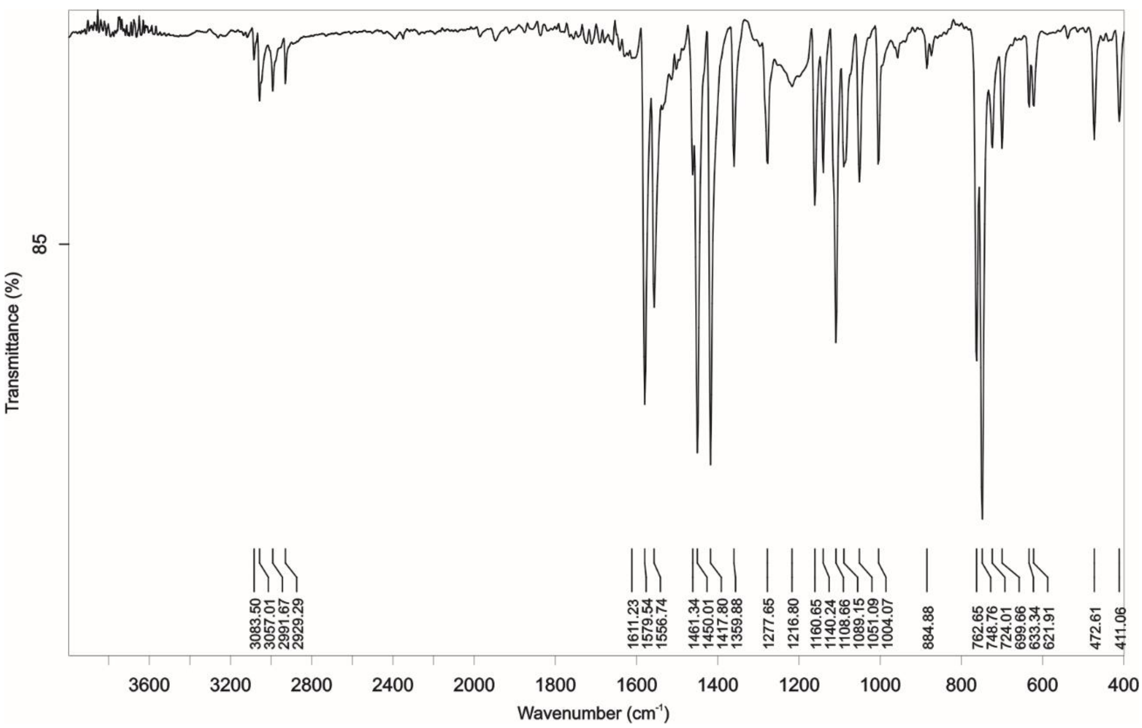

Figure S23. FT-IR spectrum of $[Cu_4I_4(L1)_2]$ (**2**).

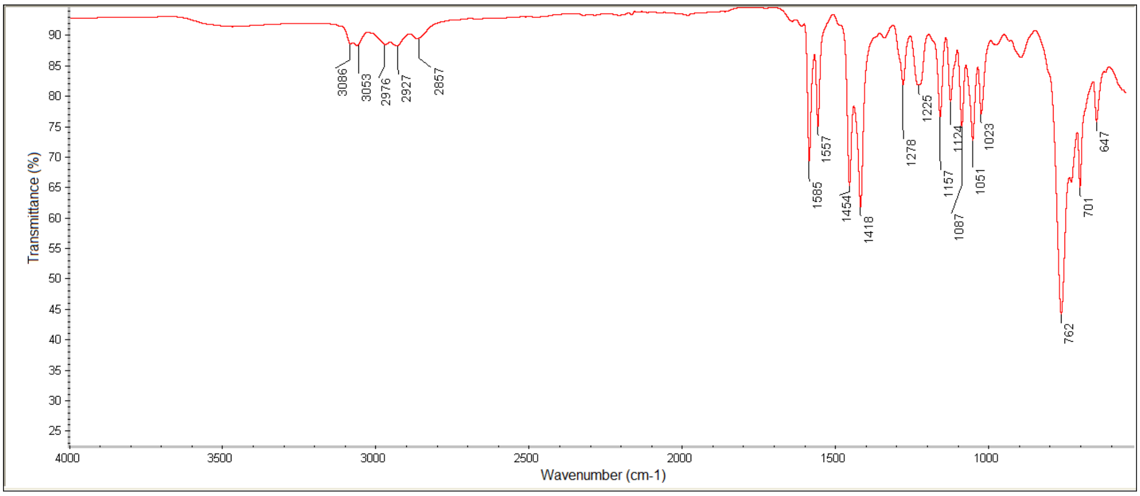

Figure S24. FT-IR spectrum of $[CuCl_2(L2)_2]$ (**3**).

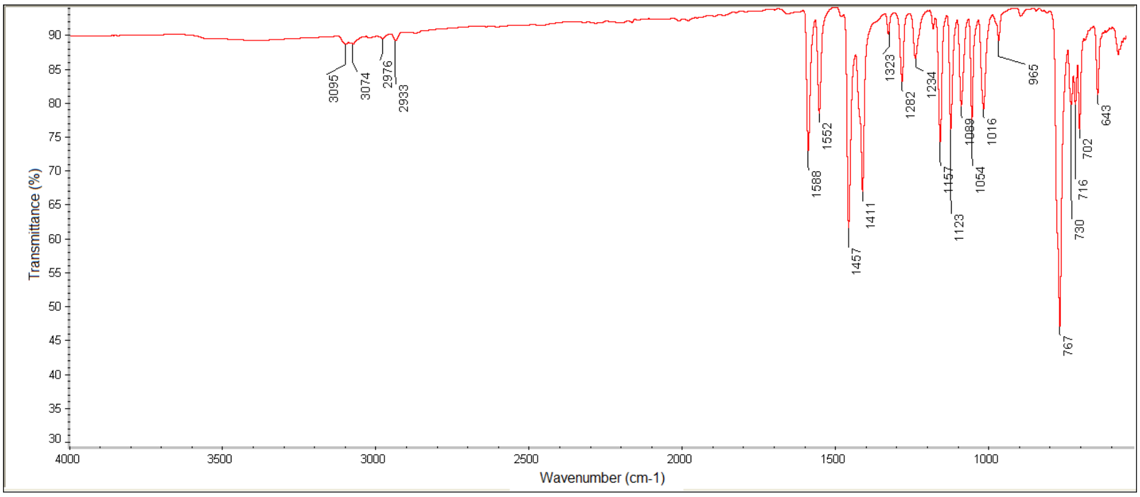

Figure S25. FT-IR spectrum of $[CoCl_2(L2)]_n$ (**4**).

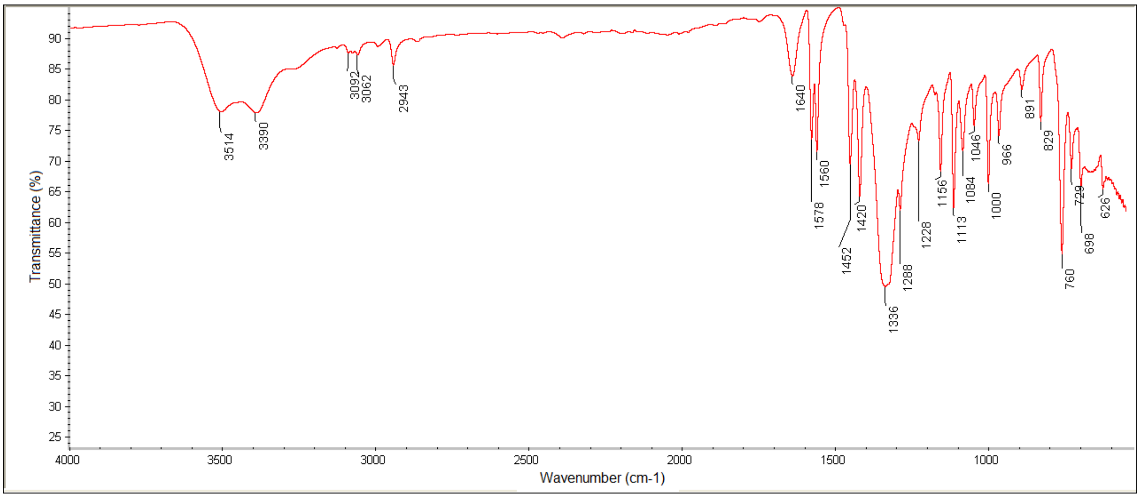

Figure S26. FT-IR spectrum of $[Ag(L2)(NO_3)]_n$ (**5**).

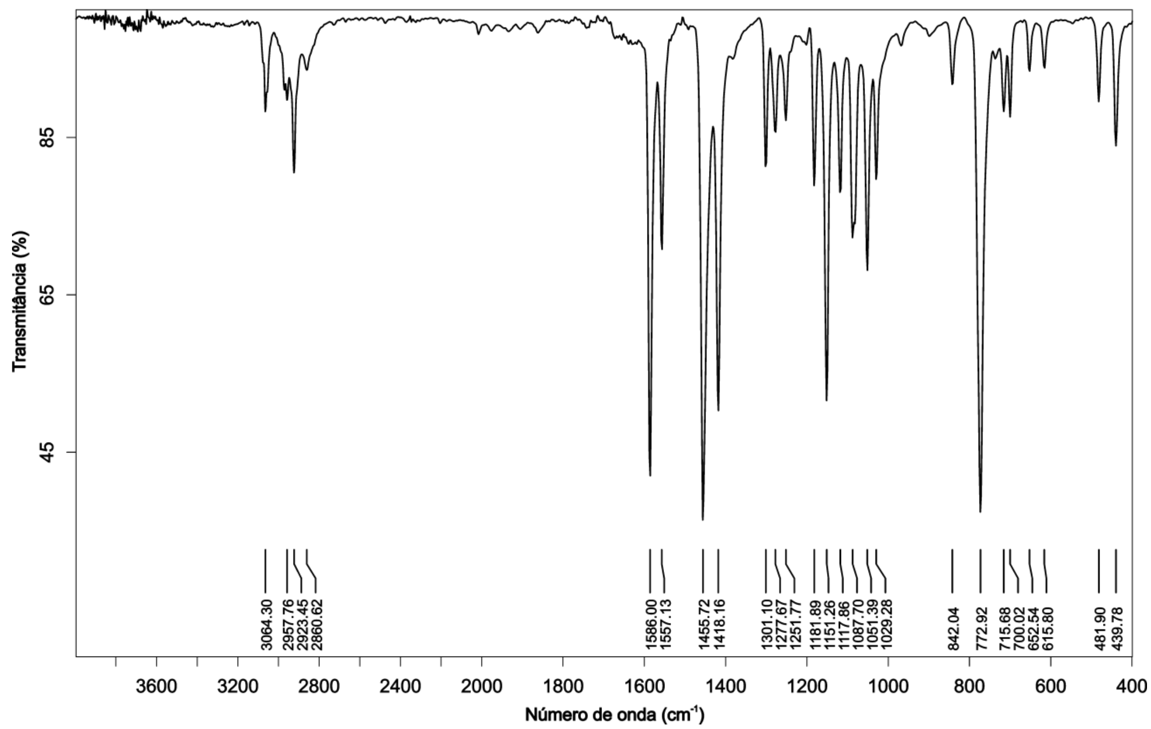

Figure S27. FT-IR spectrum of [$CuCl_2$(L3)]$_n$ (**6**).

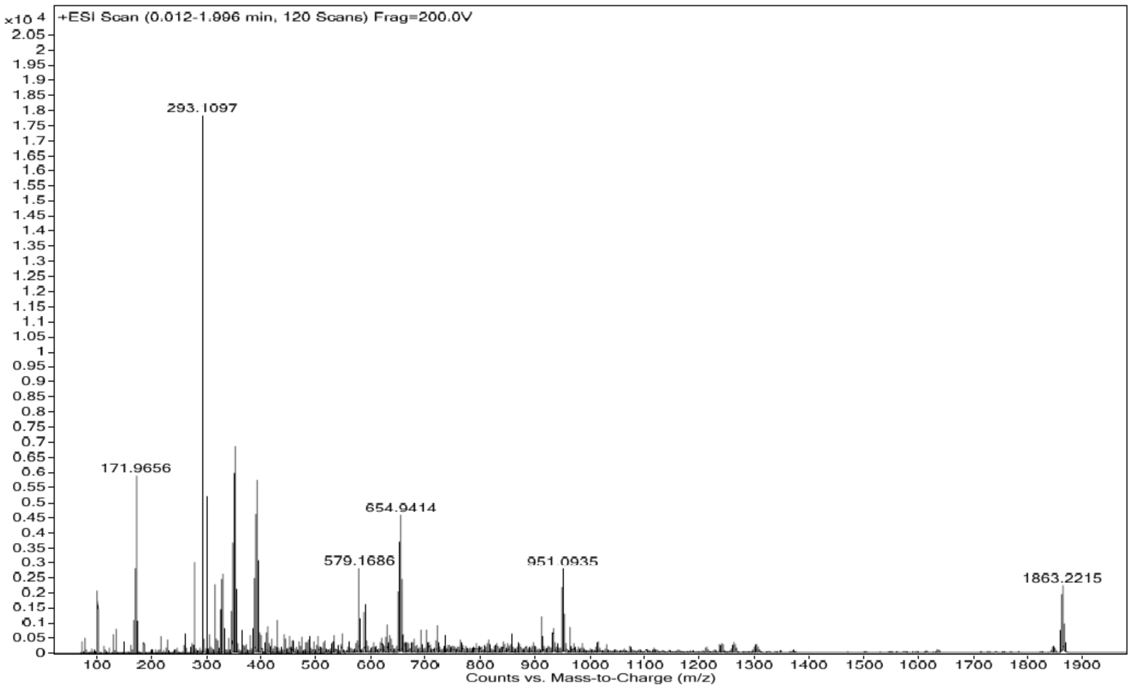

Figure S28. ESI+ MS spectrum of $[CuCl_2(L1)]_n$ (**1**).

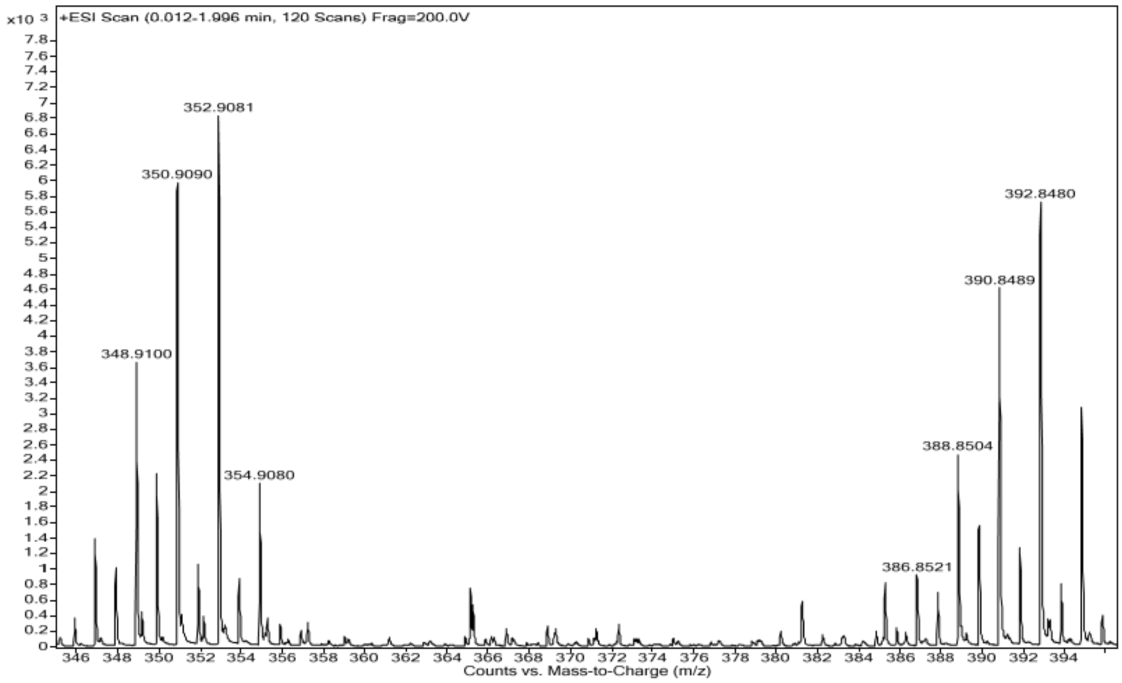

Figure S29. Expansion of the mass spectra for the compound $[CuCl_2(L1)]_n$ (**1**).

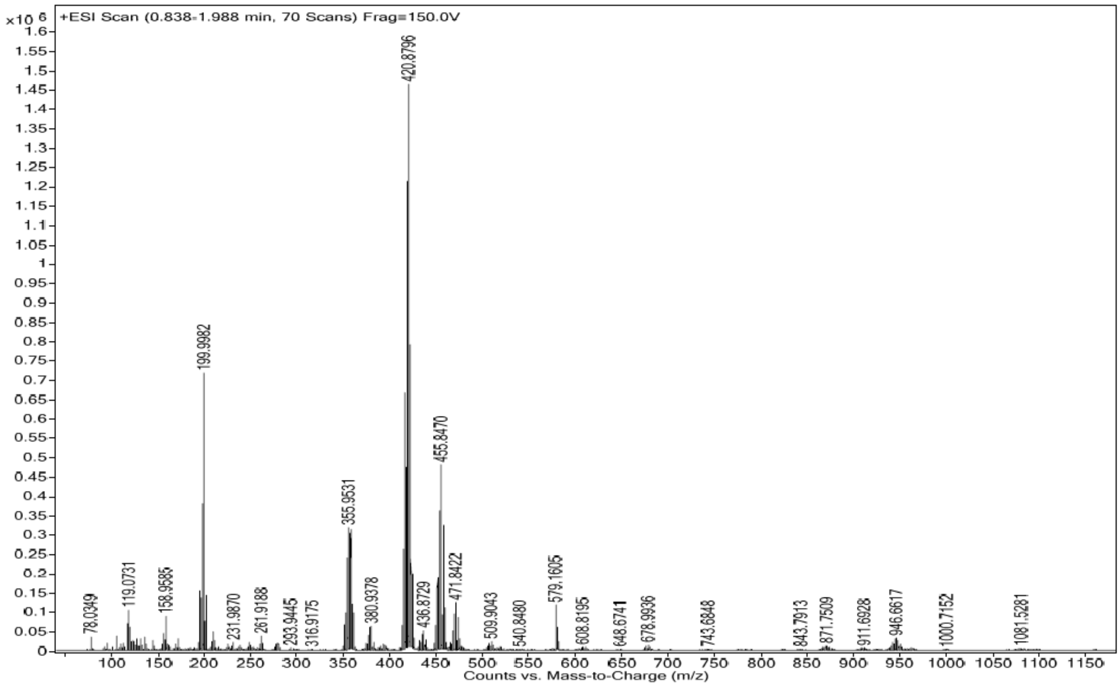

Figure S30. ESI+ MS spectrum of $[CuCl_2(L2)_2]$ (**3**).

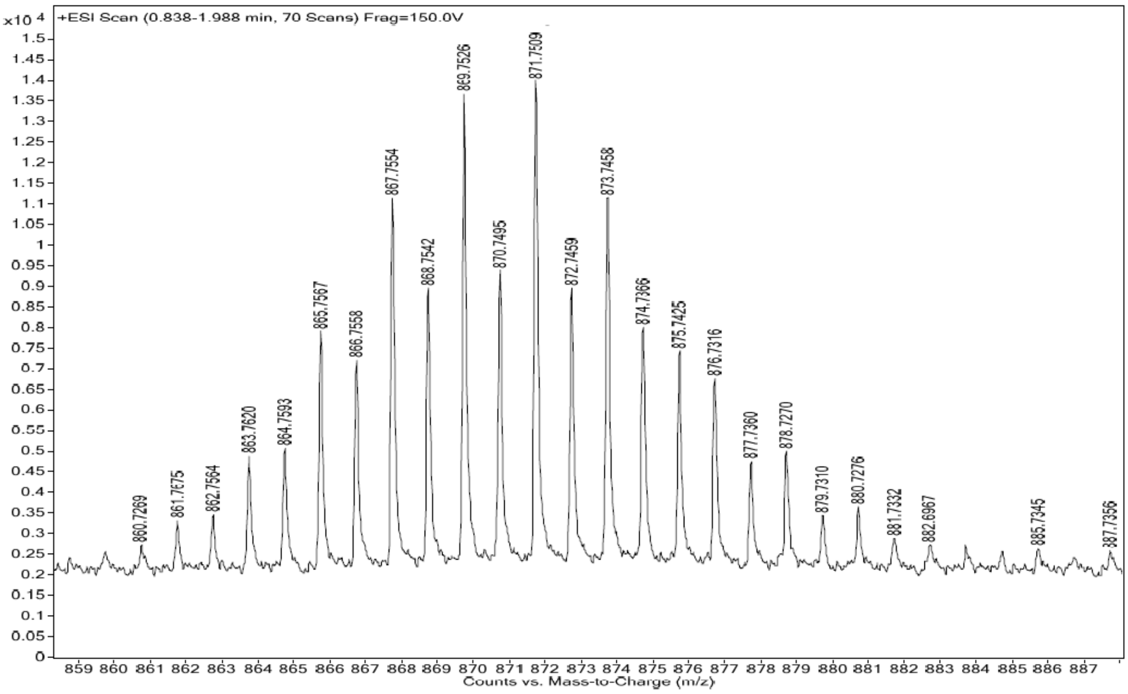

Figure S31. Expansion of the mass spectra for the compound $[CuCl_2(L2)_2]$ (**3**).

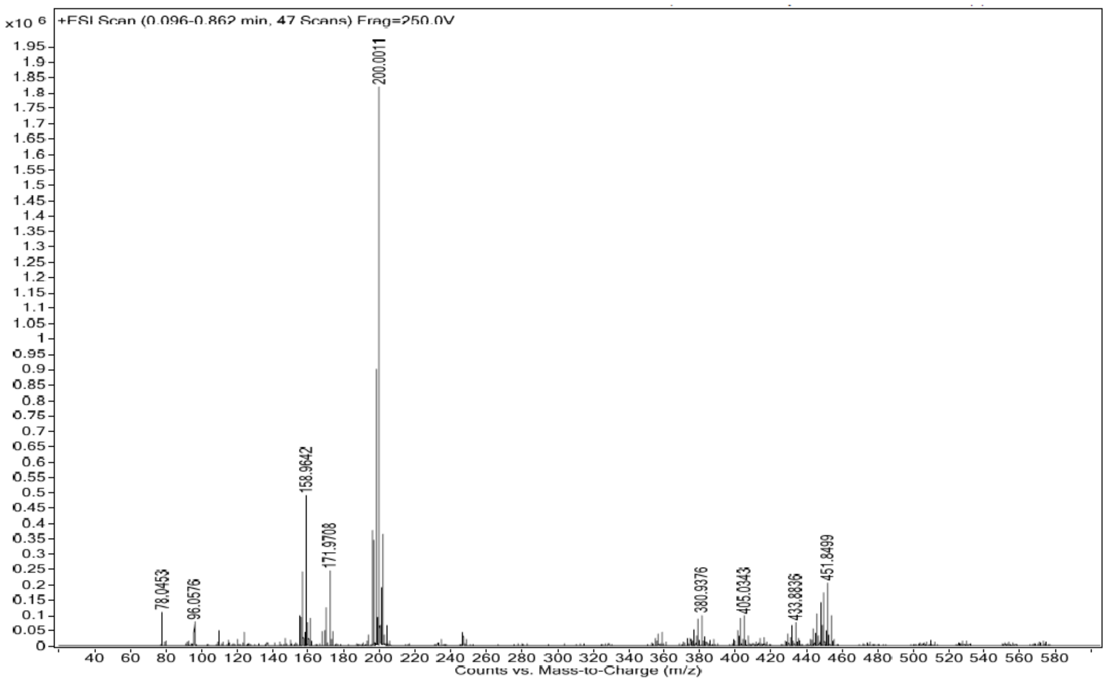

Figure S32. ESI+ MS spectrum of $[CoCl_2(L2)]_n$ (**4**).

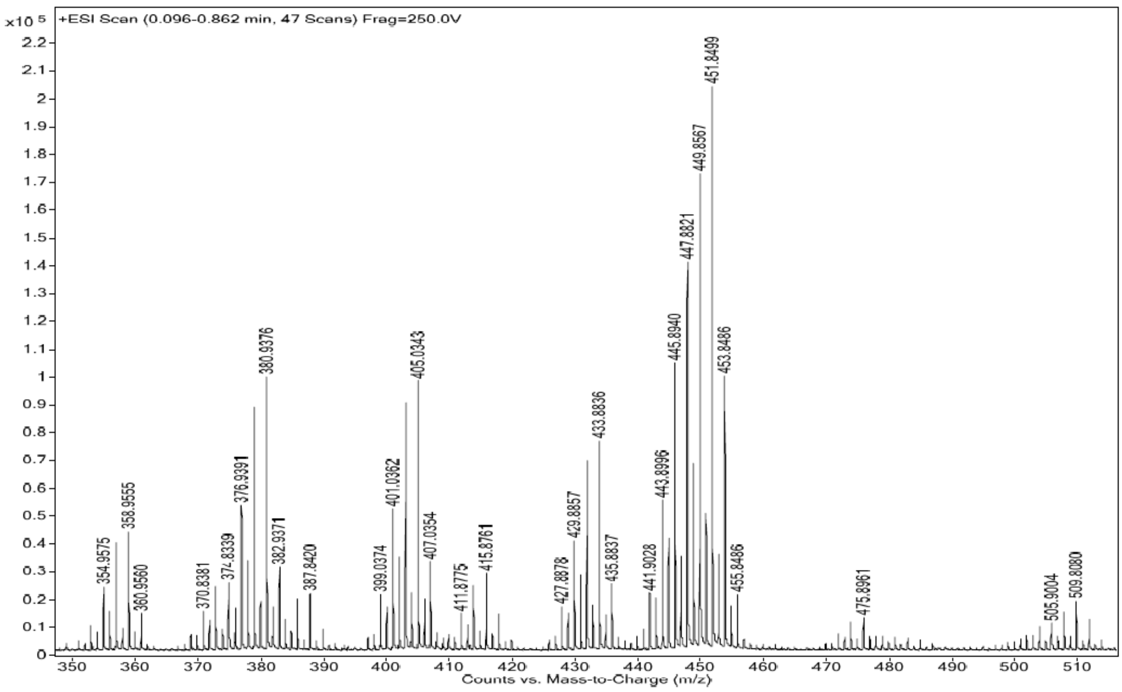

Figure S33. Expansion of the mass spectra for the compound $[CoCl_2(L2)]_n$ (**4**).

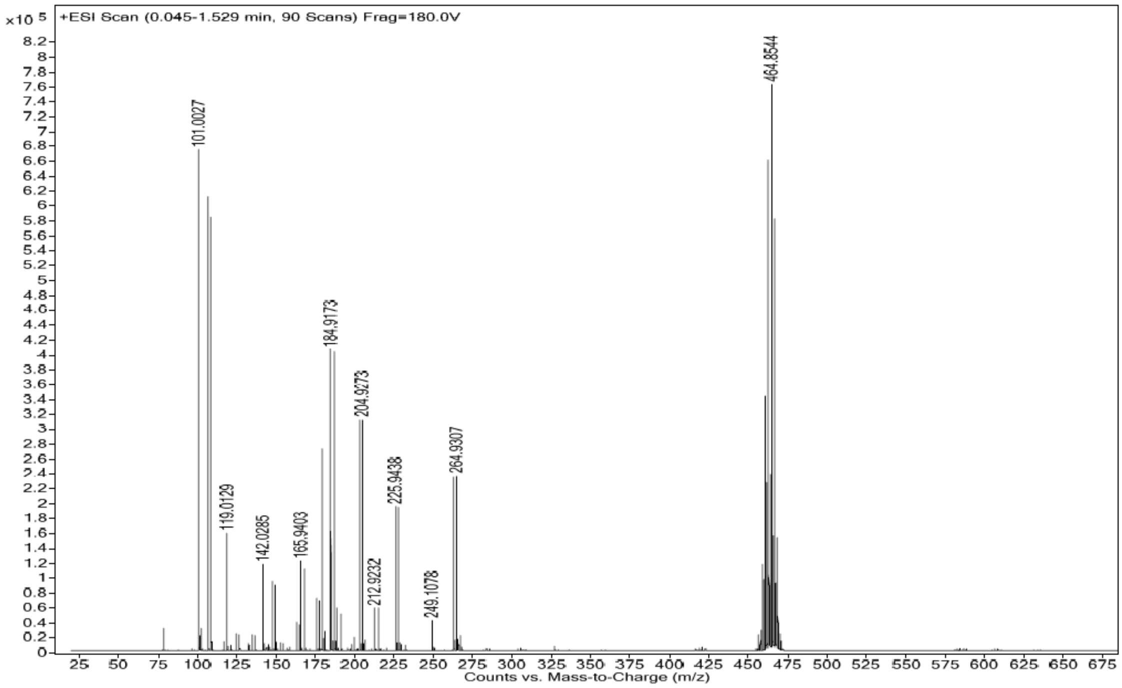

Figure S34. ESI+ MS spectrum of $[Ag(L2)(NO_3)]_n$ (**5**).

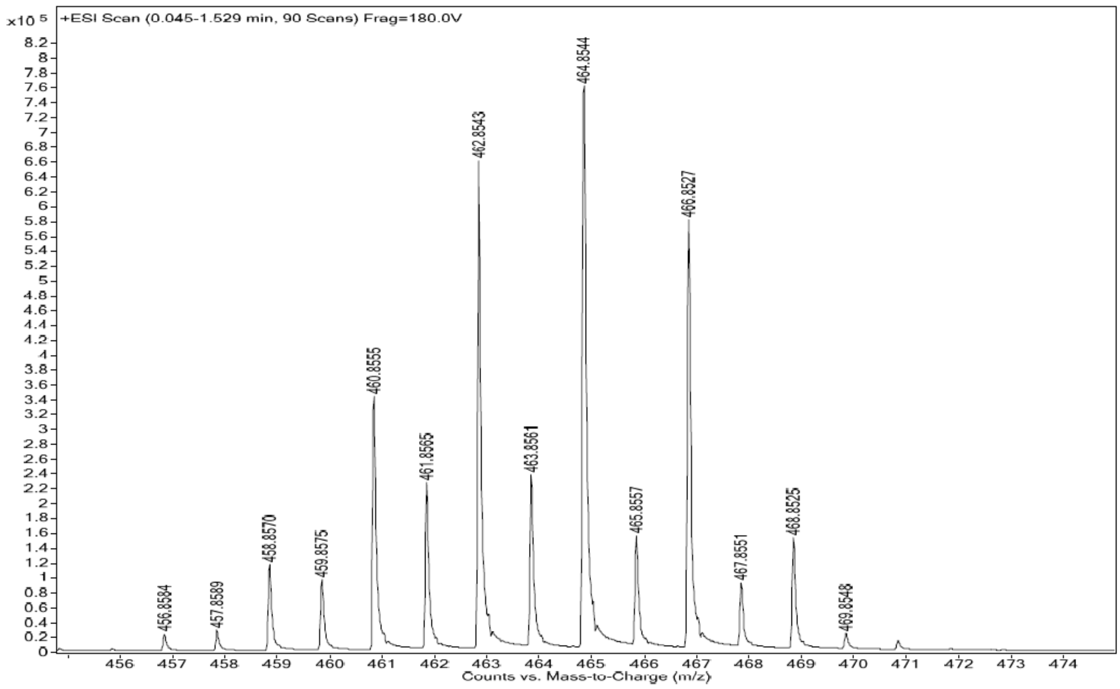

Figure S35. Expansion of the mass spectra for the compound $[Ag(L2)(NO_3)]_n$ (**5**).

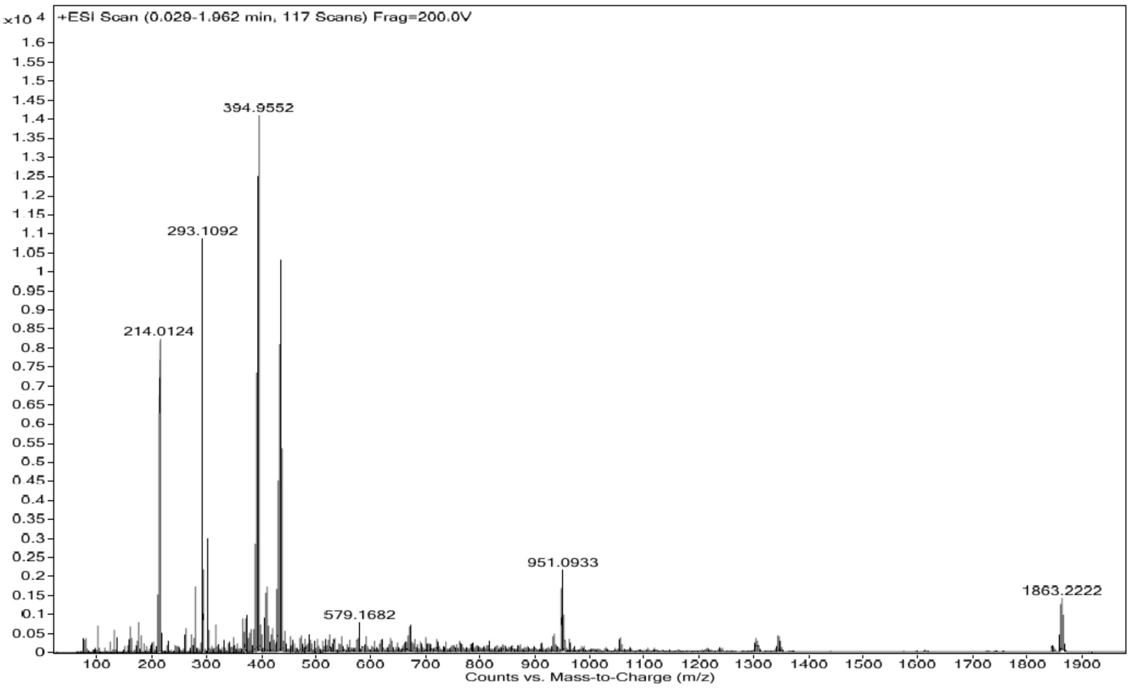

Figure S36. ESI+ MS spectrum of $[CuCl_2(L3)]_n$ (**6**).

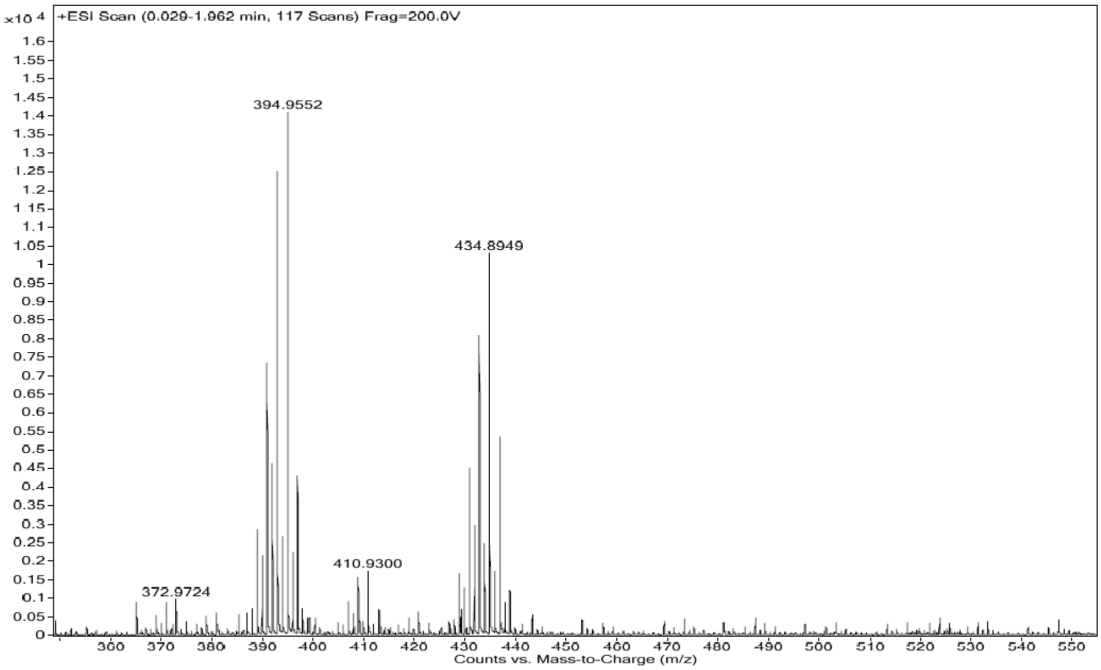

Figure S37. Expansion of the mass spectra for the compound $[CuCl_2(L3)]_n$ (**6**).